Journal of King Saud University - Science 36 (2024) 103325

HOSTED BY

Contents lists available at ScienceDirect

Journal of King Saud University - Science

journal homepage: www.sciencedirect.com

Wavelet-based digital pulse-shape method for discrimination between neutron and gamma-rays with organic scintillation detectors

Thamer Alharbi

Department of Physics, College of Science in Zulfi, Majmaah University, Majmaah 11932, Saudi Arabia

ARTICLE INFO

Keywords:
Neutron detectors
Pulse-shape discrimination

ABSTRACT

Organic scintillator detectors are central instruments in many applications involving fast neutrons. Many organic scintillator detectors exhibit pulse-shape discrimination (PSD) properties and are widely used to discriminate between neutron events and background gamma rays. PSD methods have been traditionally implemented using analog electronic circuits; however, in recent years, digital techniques have proven to outperform analog methods in areas such as count rate capability. Many digital PSD algorithms with various levels of achievement have been proposed, and those based on the wavelet transform of digitized scintillation pulses have shown great promise for operation at high event rates, where the pulse pile-up effect limits the performance of PSD methods. However, the proposed wavelet-based PSD methods involve intricate calculations that limit their practical use. In this work, we describe a modified version of the wavelet-based PSD methods that offers significant simplification of the PSD process while still producing excellent PSD performance. The method employs the Haar wavelet transform, which is the simplest available wavelet function and is easily implemented on digital hardware, such as field-programmable gate arrays (FPGA). We describe the details of the method, and different aspects of its performance are experimentally demonstrated using an experimental setup comprising a NE213 liquid scintillation detector. A figure-of-merit (FOM) of 1.47 $\pm$ 0.07 is achieved with an energy threshold of 500 keVee (electron equivalent energy). An excellent FOM value (1.32) is achieved with a short pulse processing window of only 26 ns, indicating the resilience of the method against the pulse pile-up effect.

1. Introduction

Organic scintillator detectors are ubiquitous in different fields of nuclear science and technology where fast neutron measurements are required. Examples include nuclear physics experiments (Söderström et al., 2008), fusion research (Pereira et al., 2018), oil and gas exploration measurements (Mercer et al., 2007), neutron imaging (Nattress et al., 2023), and nuclear security (Meert et al., 2022). However, neutron fields are always polluted with gamma rays emitted from the neutron source or produced by the interaction of neutrons with the surroundings. Organic scintillator detectors act in response to both gamma rays and neutrons; therefore, the measurement of fast neutrons can be significantly contaminated by contributions from background gamma rays. Fortunately, a precise measurement of neutrons is still possible based on the fact that many of the organic scintillators produce output scintillation pulses of different shapes for gamma rays and neutrons. The variations in the shapes of the gamma-ray and neutron pulses lies in their different decay-time constants, where the slow component of the scintillation light pulse for neutron events is larger than that for gamma-ray events of the same energy (Knoll, 2010). The difference in the shapes of the output light pulses is extracted using a dedicated electronic pulse processing system to distinguish neutron pulses from gamma-ray pulses, thereby producing a clean neutron response. Techniques that extract information regarding these differences are called pulse-shape discrimination (PSD) techniques (Knoll, 2010).

PSD techniques were initially implemented in analog electronic circuits. However, PSD techniques are now commonly performed using digital signal processing techniques. In digital PSD systems, the output scintillation pulses of the detectors are directly digitized with a fast waveform digitizer, and the digitized pulses are numerically processed using suitable mathematical algorithms to extract the available information on the type of incident radiation. As opposed to traditional analog PSD methods, digital techniques offer the advantage of remarkable flexibility in the choice of the PSD algorithm. Therefore, many complex methods that are not easily implementable on analog circuits can be reliably implemented on digital processors, leading to much higher precision in the analysis of a detector's output signals (Nakhostin, 2017). Wavelet transform (WT) is a powerful digital PSD technique that

E-mail address: t.alharbi@mu.edu.sa.

https://doi.org/10.1016/j.jksus.2024.103325
Received 18 February 2024; Received in revised form 19 June 2024; Accepted 24 June 2024
Available online 26 June 2024

has been successfully used with organic scintillator detectors (Langeveld et al., 2017; Langeveld et al., 2020; Singh and Mehra, 2017; Singh and Singh, 2015; Yang et al., 2014; Yousefi et al., 2009). In wavelet-based PSD techniques, the wavelet transform of the scintillation pulses is first calculated, and information on the type of incident particle is obtained by mathematical processing of the result. The advantages of wavelet-based PSD techniques include good PSD performance and resilience to the pulse pile-up effect (Langeveld et al., 2017; Langeveld et al., 2020; Singh and Mehra, 2017; Yang et al., 2014). However, determining the type of radiation from the wavelet transform of the pulses requires the execution of a significant amount of optimization and computations, which limits the practical use of these methods. In this work, we report a new wavelet-based PSD method that, in addition to excellent PSD performance, significantly simplifies the PSD procedure for liquid scintillation detectors. We present the method in detail and demonstrate its excellent operation using an experimental setup.

2. Wavelet transform

Here, we briefly describe the principles of the wavelet transform. Further details can be found in Debnath (2001). The wavelet transform is an evolution of the common Fourier transform. The Fourier transform of a signal provides information on its frequency components over the entire duration of the signal. However, it does not provide information regarding the time locations of the frequency components in the signal. The wavelet transform facilitates the analysis of a signal simultaneously over both time and frequency, whereas the Fourier transform only analyzes a signal in the frequency domain. In the wavelet transform, the time and frequency information of the signal are simultaneously produced using the so-called mother wavelet function. The mother wavelet function is scaled, shifted, and then convolved with the signal. Frequency information is obtained by varying the scale value, whereas time information is obtained by varying the shift value. The wavelet function for every scale (s) and shift value (u) of the mother wavelet ϕ is given by

$$\varphi_{u,s} = \frac{1}{\sqrt{s}}\varphi\left(\frac{t-u}{s}\right) \tag{1}$$

where t is the time. The wavelet transform of a signal $f(t)$ at shift u and scale s is defined as

$$Wf(u,s) = \frac{1}{\sqrt{s}}\int_{-\infty}^{\infty} \varphi^{*}\left(\frac{t-u}{s}\right) f(t)dt \tag{2}$$

where the stat implies the complex conjugate. Many types of mother wavelet functions (ϕ) are available, but the best one is generally selected based on the application and type of information that needs to be extracted from the signal. Various wavelet functions have been investigated for PSD applications using organic scintillator detectors. For instance, Yousefi et al. (2009) used the Haar wavelet function, which is the most uncomplicated available mother wavelet function. Singh and Mehra (2017) examined a wide range of mother wavelets regarding their resilience to the pulse-pile-up effect.

3. New pulse-shape discrimination method

An organic scintillator detector is composed of an organic scintillator material attached to a light-to-electric signal converter device such as a photomultiplier tube. In previously reported wavelet-based PSD methods, the wavelet transform of a digitized photomultiplier pulse is obtained and mathematically processed to extract a parameter that determines the type of incident particle. This parameter is called the PSD parameter or discrimination parameter. The main novelty of the proposed approach is that the PSD parameter is directly extracted from the amplitude of the wavelet transforms of the pulses, and no further mathematical processing of the wavelet transforms is required. To this end, the digitized photomultiplier pulses are first numerically integrated, and then a wavelet transform is applied to the integrated pulses in lieu of the photomultiplier pulses. This slight modification significantly simplifies the PSD process, with two further advantages:

(i) The integration of photomultiplier pulses transforms gamma-ray and neutron pulses of different decay-time constants into pulses of different curvatures at their leading edges. It has already been demonstrated that the Haar wavelet function is very powerful for detecting variations in the curvature (rise time) of signals (Tang, 2014). Therefore, the Haar wavelet can be optimally used in the proposed method. As mentioned previously, the Haar wavelet transform is the simplest and easiest wavelet to implement in a digital processor.

(ii) The integration of the photomultiplier pulse reduces noise in the pulses. In particular, quantization noise, which is significant when digitizers with a low resolution (e.g., 8-bit) are used, covers a wide energy range. Therefore, good performance is expected in the presence of noise.

Fig. 1 illustrates the proposed PSD method. Synthetic gamma-ray and neutron pulses are shown in the top panel of the figure. Synthetic pulses were generated using the pulse models for the NE213 scintillator detector described in Marrone et al. (2002). Two pulses of the same amplitude exhibited different decay-time constants, whereas the neutron pulse exhibited a larger decay-time constant. The integrated pulses are shown in the middle panel of the figure. The integrated pulses are normalized to their amplitudes. The pulse integration was performed numerically using the following simple recursive formula:

$$Output[n] = Output[n-1] + Input[n] \tag{3}$$

where *Output* is the integrated pulse, *Input* is the digitized pulse, and n is the sample number. One can clearly see a difference in the curvature of the integrated pulses, although both pulses have the same amplitude. The height of the scintillation pulse after the integration represents the energy (light output) of the event. Haar wavelet transforms of the integrated pulses are shown at the bottom of the figure. The Haar wavelet was obtained using the *cwt* built-in function in MATLAB (version R2020a). As discussed in Section 2, a choice of the scale value is required for the calculation of a wavelet transform. As shown in Fig. 1, the wavelet transforms were calculated by adopting a typical scale value of 30 ns. The Haar Wavelet transforms have significantly different amplitudes for gamma-ray and neutron events. Therefore, a direct comparison of the amplitude of the wavelet transform with the energy of the event can be readily used as a discrimination parameter (PSD parameter), with no further computations required.

4. Experimental setup

The data were collected using the experimental setup described in our previous study (Alharbi, 2019). The setup included a NE213 liquid scintillation detector (5.08 cm × 5.08 cm) coupled to a photomultiplier tube model R329 Hamamatsu. The negative voltage applied to the photomultiplier tube was − 1500 V and the output pulses from the anode of the photomultiplier tube were directly fed into a fast digital oscilloscope with a sampling rate of 5 GSample/s and 8-bit resolution. The output pulses were recorded using an americium–beryllium (Am–Be) neutron source with an activity of (~1 GBq). The Am–Be neutron source emits neutrons from an (α,n) reaction. Gamma rays are mainly emitted from the americium component. Some gamma rays are also produced because of the inelastic scattering of fast neutrons from the surroundings. Approximately 40,000 pulses were recorded using a digital oscilloscope. The digitized pulses were processed offline on a personal computer using a script written in MATLAB. Each pulse was recorded within a time window of 250 ns. Measurements with standard laboratory gamma-ray sources, such as ^{22}Na and ^{137}Cs, were also

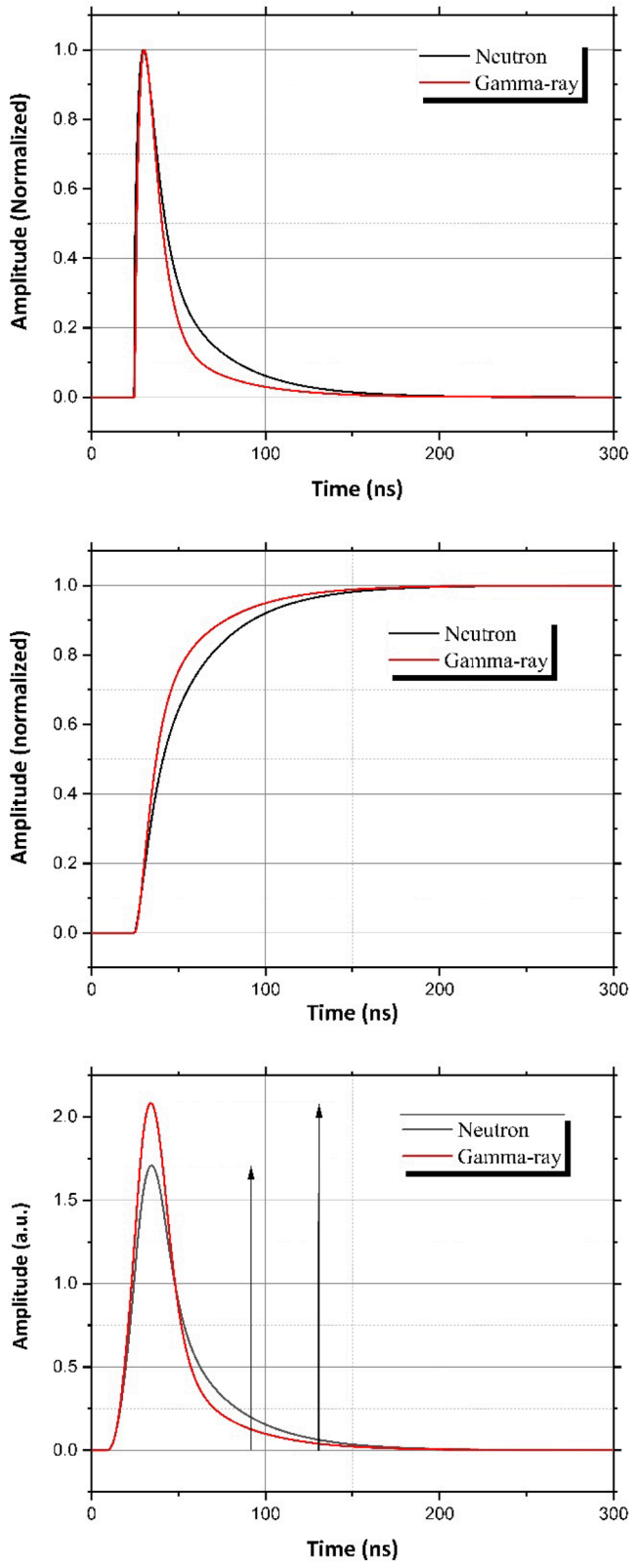

Fig. 1. (Top) Calculated gamma-ray and neutron pulses for the NE213 liquid scintillation detector. (Middle) The integrated pulses, after normalization to their amplitudes. The amplitude-normalized integrated pulses show different degrees of curvature in their leading-edges. (Bottom) Wavelet transforms of the pulses. The amplitude of the wavelet transforms is different whereas the amplitudes (energy) of the original pulses are the same. The arrows represent the amplitudes of the pulses.

performed for energy calibration of the system.

5. Experimental results

5.1. Energy calibration

The energy scale (light output) of the system was first calibrated using pulses collected from the ^{22}Na and ^{137}Cs gamma-ray sources. For this purpose, the offset in the baseline of each scintillation pulse was first adjusted to zero by subtracting the average values of the samples before the start of the pulse, as determined by the oscilloscope's trigger level (samples at the baseline of the pulse), from the entire pulse. The photomultiplier scintillation pulses were numerically integrated using Eq. (3). The amplitude of the integrated pulse is proportional to the total scintillation light released in the detector, which is proportional to the total energy deposition inside the detector. Owing to the low atomic number of organic scintillators, the energy spectrum of gamma rays mainly results from the Compton scattering of gamma rays from the organic material. Nevertheless, the Compton edges in the energy spectra can be used to calibrate the light output. Energy calibration was carried out by considering a channel number corresponding to 75 % of the amplitude of the Compton edge, as discussed in Cherubini (1989). The energy spectra of ^{22}Na and ^{137}Cs gamma-ray sources are shown in Fig. 2. The Compton edges in the spectra correspond to 341 and 1062 keVee for ^{22}Na, and 477 keVee for ^{137}Cs. The lower-level energy threshold of the system is approximately 80 keVee (electron-equivalent energy). The upper energy level of the system reaches approximately 2000 keVee, above which the input range of the oscilloscope is saturated and the pulses are not recorded properly.

5.2. Neutron and gamma-ray discrimination

Fig. 3 represents the discrimination parameter as a scatterplot versus the energy (light output) of the events. Pulses saturated by the input range of the oscilloscope were excluded from the pulse processing program. The discrimination between gamma-ray and neutron events is apparent. For comparison, the results of the PSD process applied to events collected with the ^{137}Cs gamma-ray source are also shown. The discrimination parameter was calculated as the ratio of the maximum value of the Haar wavelet transform to the light output of the pulse, that is, the amplitude of the pulse after integration. A typical scale value of 10 ns was used for the Haar wavelet transform calculations. As can be

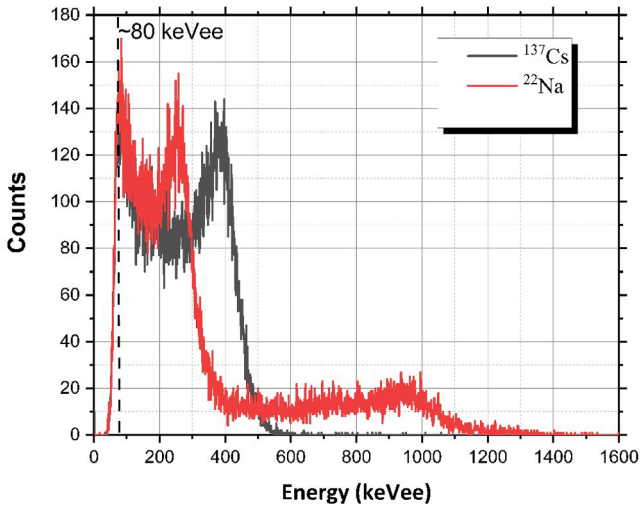

Fig. 2. Calibrated energy spectra of ^{137}Cs and ^{22}Na. The calibration was achieved by using the Compton edges in the spectra (341 and 1062 keVee for ^{22}Na and 477 keVee for ^{137}Cs). The energy threshold of the system lies at approximately 80 keVee.

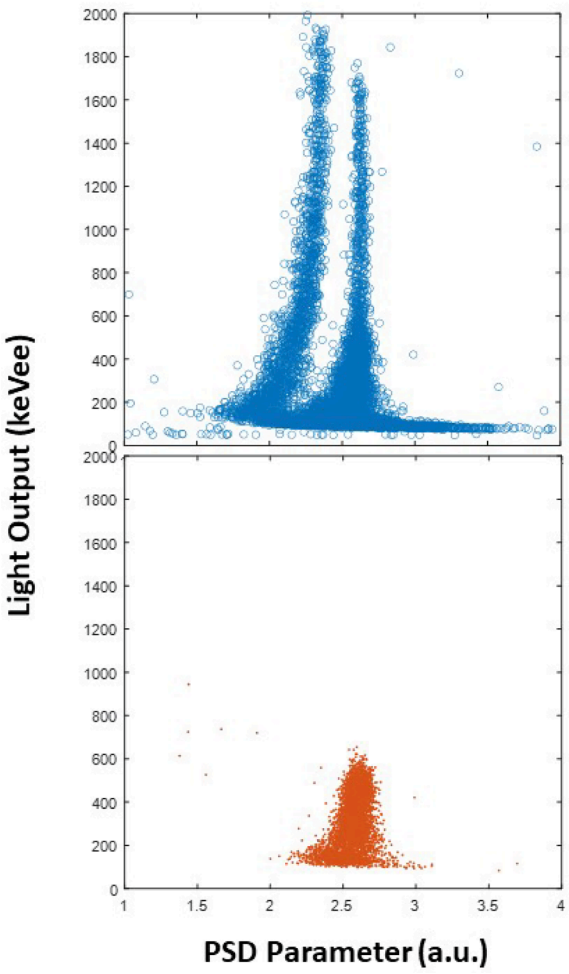

Fig. 3. Scatter plots of the pulse-shape discrimination (PSD) parameter against the light output for events recorded with the Am–Be neutron source (top) and ^{137}Cs gamma-ray source (Bottom). A clear discrimination of gamma-ray and neutron events is achieved with the new wavelet-based PSD method, down to a light output of approximately 100 keVee.

observed, the gamma-ray and neutron events lie in two separate plumes. The events in the right-side plume represent gamma rays, whereas those in the left-side plume correspond to neutrons. This behavior is explained by the fact that, for events with the same light output, a faster rise time of the integrated gamma-ray pulses produces a Haar wavelet transform with a larger amplitude.

A figure-of-merit (FOM) parameter is commonly utilized to quantify the quality of discrimination between different events (Winyard et al., 1971). The FOM is calculated from a histogram of the discrimination parameters. The histogram shows two peaks related to the gamma-ray and neutron events. If these peaks are Gaussian in shape, the FOM is defined in terms of the distance between the centers of the peaks and the full width at half maximum (FWHM) of the two Gaussian peaks:

$$FOM = \frac{D}{FWHM_n + FWHM_\gamma} \tag{4}$$

where D is the distance between the centroids of the gamma-ray and neutron peaks in the histogram of the discrimination parameter. FWHM$_n$ and FWHMγ are the FWHMs of the gamma-ray and neutron peaks, respectively. These parameters are extracted by fitting a double Gaussian function to a histogram of the discrimination parameters. A high FOM value indicates good separation of gamma-ray and neutron events. The FOM values were calculated using the data shown in Fig. 3.

A histogram of the discrimination parameter, together with the double Gaussian fit for events with energies above 500 keVee, is shown in Fig. 4. For an accurate calculation of the FOM, the distribution of the PSD parameters of the events must exhibit a good Gaussian shape (Langeveld et al., 2017). Therefore, an energy threshold of 500 keV was selected because the peaks in the histogram of the PSD parameters of the events above this threshold showed relatively good Gaussian shapes. This threshold value is also the same as that used in previous works cited in Section 5.4 for comparison. The fit of a double Gaussian function results in the following fitting parameters: FWHMn = 15.66 ± 0.50, FWHMγ = 6.43 ± 0.30, and D = 32.6 ± 0.80, from which a FOM = 1.47 ± 0.07 is calculated. It has already been shown that the complete separation of gamma-ray and neutron events is practically achieved with an FOM value greater than 1.27 (Zaitseva et al., 2012). According to this baseline, our PSD method leads to the complete separation of gamma-ray and neutron events with an energy threshold value of 500 keVee. Nevertheless, it is visually observable in Fig. 3 that some discrimination is still attained down to approximately 100 keVee.

As previously mentioned, a scale value should be selected for the calculation of the Haar wavelet transform of the integrated photomultiplier pulses. The effect of the scale value on the PSD performance of the method was assessed by calculating the FOM for different scale values. Fig. 5 shows the behavior of the FOM as a function of the scale value in the Haar wavelet transform. The discrimination performance initially improves with increasing scale value. The optimal scale value corresponding to the highest FOM is approximately 10 ns. Upon further increase in the scale value, the FOM decreases very slowly.

5.3. *Effect of the pulse processing window*

Another test that we performed on the PSD algorithm was the dependency of the PSD performance on the size of the pulse processing window. The size of the pulse processing window is crucial from the perspective of pulse pile-up because a short pulse processing window is desired to reduce the effect of interference from successive events. Fig. 6 represents the dependence of the FOM on the duration of the pulse processing window. In these calculations, the length of the pulse processing window was reduced in steps of 10 ns, and each pulse processing window contained 30 samples (equal to 6 ns) of the pulse baseline. Even with a short pulse processing window of 26 ns, good discrimination with an FOM value of 1.32 was attained. When the pulse processing window was reduced to 16 ns, the FOM decreased to 0.6, indicating that some

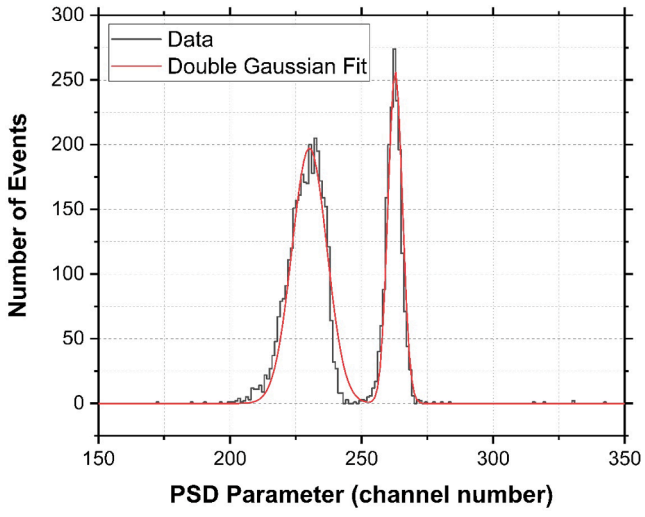

Fig. 4. Results of the figure-of-merit (FOM) calculations for the events above an energy threshold of 500 keVee. The distribution of the PSD parameter together with the double Gaussian fit is shown. An excellent FOM value of 1.47 ± 0.07 is achieved.

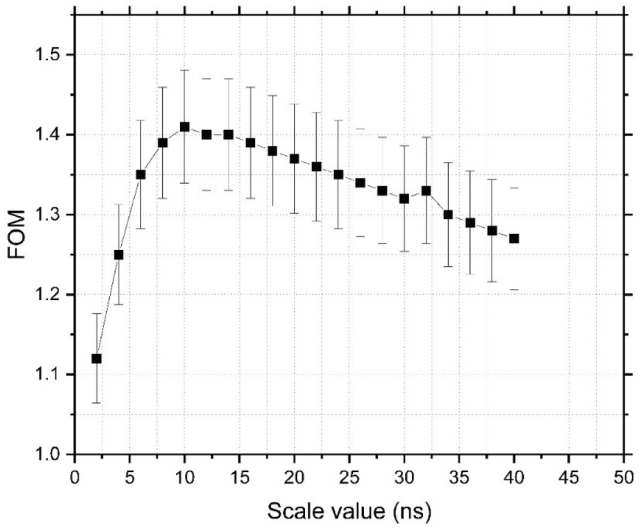

Fig. 5. Variations of the FOM value with the scale value of the Haar wavelet transform function. The best PSD performance is achieved with a scale value of approximately 10 ns.

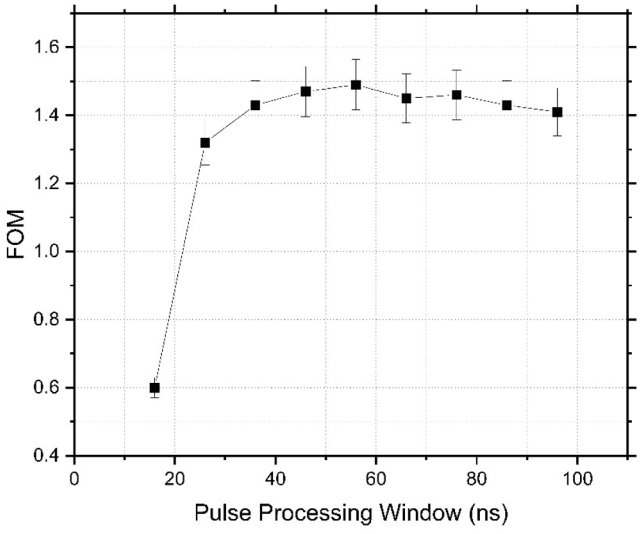

Fig. 6. Dependence of the FOM value on the length of the pulse processing window.

discrimination between events could still be achieved with such a short pulse processing window. These results are promising for PSD in high-rate applications.

5.4. Comparison with other wavelet-based methods

The typical duration of scintillation pulses from liquid scintillator detectors is 200–300 ns (Kaschuck and Esposito, 2005; Prusachenko et al., 2018). However, as mentioned earlier, from a pulse pile-up perspective, it is highly desirable to identify the type of particle early in the pulse lifetime, that is, by using a short pulse processing window. The minimum length of the pulse processing window for standard PSD methods, such as the charge comparison method, is 80–120 ns (Kaschuck and Esposito, 2005; Nakhostin, 2020). The main advantage of wavelet-based PSD methods is that they are not demanding in terms of the length of the pulse processing window. Table 1 presents a comparison of our PSD method with previous wavelet-based methods as well as the standard charge-comparison method. The energy threshold for all the methods was 500 keVee. The proposed method is superior in terms of both the minimum necessary length of the pulse processing window and the corresponding FOM value.

Table 1
Length of the pulse processing window and the corresponding FOM values of the various wavelet-based PSD methods together with the result of the standard charge-comparison method.

Method	Time Window	FOM	Reference
Haar Wavelet	40 ns	0.28	Singh and Mehra (2017)
Daubechies Wavelet	40 ns	0.98	Singh and Mehra (2017)
Symlets Wavelet	40 ns	0.99	Singh and Mehra (2017)
Coiflet Wavelet	40 ns	0.98	Singh and Mehra (2017)
Charge-Comparison	50 ns	0	Nakhostin (2020)
Charge-Comparison	88 ns	1.23	Nakhostin (2020)
Pulse integration Pulse Haar Wavelet	26 ns	1.32	Present Work

6. Discussion

The method presented in this paper is an evolution of previously reported wavelet-based PSD methods (Langeveld et al., 2017; Langeveld et al., 2020; Singh and Mehra, 2017; Singh and Singh, 2015; Yang et al., 2014; Yousefi et al., 2009). By adding a simple integration of photomultiplier pulses before taking the wavelet transform, the following advantages can be achieved:

- This method simplifies the PSD process because we can use the Haar wavelet function, which is the most straightforward available wavelet function, and the PSD parameter is simply obtained through an amplitude comparison. For the extraction of a PSD parameter using the method presented by Yousefi et al. (2009) a calculation of a scale function from the Haar wavelet transform of the pulses is required, whereas our method avoids any further processing of the wavelet transforms. The method presented by Singh and Mehra (Singh and Mehra, 2017; Singh and Singh, 2015) employs more complex wavelet functions, whereas the Haar wavelet transform in our method is the simplest available wavelet function that can be readily realized on digital processors such as field-programmable gate arrays (FPGA) (Sarkar and Bhairannawar, 2021).
- The method produces an excellent PSD performance as quantified with a FOM value of 1.47 $\pm$ 0.07 for an energy threshold of 500 keVee, which can be considered as a complete separation of gamma rays and neuton.
- Excellent PSD can be achieved when the duration of the pulse acquisition window is as short as 26 ns, which significantly reduces the sensitivity of the system to the pulse pile-up effect. This is a significant improvement over previous PSD methods and is very promising for high-rate applications, such as nuclear security and fusion research (Ishikawa et al., 2006; LaGraffe, 2018).
- This method requires the optimization of only a single parameter, that is, the scale parameter in the Haar wavelet transform. This allows the convenient use of the method with various scintillators having different decay-time constants.

7. Summary and conclusion

A wavelet-based digital PSD method was developed to separate gamma-ray and neutron pulses from an organic scintillator detector. The method employs the simple Haar wavelet transform function by only adding an integration of the photomultiplier pulses to the pulse processing procedure, thereby significantly abridging the extraction of the PSD parameter compared with previously reported wavelet-based digital PSD methods. The performance of the method was experimentally studied with a NE213 liquid scintillator detector and a FOM value of 1.47 $\pm$ 0.07 was accomplished with an energy threshold of 500 keVee. The method provided excellent performance with pulse processing

windows as short as 26 ns, which can significantly reduce sensitivity to the pulse pile-up problem. This method can be easily used with any type of scintillator, as only the optimization of a single parameter of the scale value in the Haar wavelet transform function is required. The results of this study show that this method is promising for building compact digital fast neutron detector systems for applications in nuclear security, fusion research, and environmental monitoring.

CRediT authorship contribution statement

Thamer Alharbi: Writing – review & editing.

Declaration of competing interest

The authors declare that they have no known competing financial interests or personal relationships that could have appeared to influence the work reported in this paper.

Acknowledgment

The author extends the appreciation to the Deanship of Postgraduate Studies and Scientific Research at Majmaah University for funding this research work through the project number (R-2024-1163)

References

Alharbi, T., 2019. Distance metrics for digital pulse-shape discrimination of scintillator detectors. Radiat. Phys. Chem. 156, 205–209. https://doi.org/10.1016/j.radphyschem.2018.11.014.

Debnath, L., 2001. Wavelet Transforms and Their Applications, second ed. Birkhäuser Boston.

Ishikawa, M., Itoga, T., Okuji, T., Nakhostin, M., Shinohara, K., Hayashi, T., Sukegawa, A., Baba, M., Nishitani, T., 2006. Fast collimated neutron flux measurement using stilbene scintillator and flashy analog-to-digital converter in JT-60U. Rev. Sci. Instrum. 77, 10e706. https://doi.org/10.1063/1.2221927.

Kaschuck, Y., Esposito, B., 2005. Neutron/-ray digital pulse shape discrimination with organic scintillators. Nucl. Instrum. Methods Phys. Res. Sect. a. 551, 420–428. https://doi.org/10.1016/j.nima.2005.05.071.

Knoll, G.F., 2010. Radiation Detection and Measurement, fourth ed. John Wiley & Sons.

LaGraffe, D., 2018. Nuclear security science. In: Masys, A. (Ed.), Handbook of Security Science. Springer, Cham. https://doi.org/10.1007/978-3-319-51761-2_18-1.

Langeveld, W.G.J., King, M.J., Kwong, J., Wakeford, D.T., 2017. Pulse shape discrimination algorithms, figures of merit, and gamma-rejection for liquid and solid scintillators. IEEE Trans. Nucl. Sci. 64, 1801–1809. https://doi.org/10.1109/TNS.2017.2681654.

Langeveld, W.G.J., Glenn, A.M., Sheets, S.A., Strellis, D.A., Zaitseva, N.P., 2020. Comparison of pulse-shape discrimination performance of stilbene and liquid scintillator under high count-rate active interrogation conditions. Nucl. Instrum. Meth. a. 954, 161204.

Marrone, S., Cano-Ott, D., Colonna, N., Domingo, C., Gramegna, F., Gonzalez, E.M., Gunsing, F., Heil, M., Käppeler, F., Mastinu, P.F., Milazzo, P.M., Papaevangelou, T., Pavlopoulos, P., Plag, R., Reifarth, R., Tagliente, G., Tain, J.L., Wisshak, K., 2002. Pulse shape analysis of liquid scintillators for neutron studies. Nucl. Instrum. Methods Phys. Res. A 490, 299–307. https://doi.org/10.1016/S0168-9002(02)01063-X.

Meert, C.A., MacDonald, A.T., Jinia, A.J., Steinberger, W.M., Clarke, S.D., Pozzi, S.A., 2022. Photoneutron detection in active interrogation scenarios using small organic scintillators. IEEE Trans. Nucl. Sci. 69, 1397–1402. https://doi.org/10.1109/TNS.2022.3164601.

Mercer, J.A., Hussein, E.M.A., Waller, E.J., 2007. A non-intrusive neutron device for in situ detection of petroleum contamination in soil. Nucl. Instrum. Meth. b. 263, 217–220. https://doi.org/10.1016/j.nimb.2007.04.088.

Nakhostin, M., 2017. Signal Processing for Radiation Detectors. John Wiley & Sons.

Nakhostin, M., 2020. A technique for the reduction of pulse pile-up effect in pulse-shape discrimination of organic scintillation detectors. Nucl. Eng. Technol. 52, 360–365. https://doi.org/10.1016/j.net.2019.07.035.

Nattress, J.T., Hausladen, P.A., Rose Jr., P.B., 2023. Fast-neutron/gamma-ray radiography using a broad-energy neutron source. Nucl. Instrum. Meth. A 1047, 167701. https://doi.org/10.1016/j.nima.2022.167701.

Pereira, R.C., Fernandes, A., Cruz, N., Sousa, J., Riva, M., Marocco, D., Belli, F., Gonçalves, B., 2018. Neutron/Gamma discrimination code based on trapezoidal filter. Fusion Eng. Des. 134, 118–122. https://doi.org/10.1016/j.fusengdes.2018.07.002.

Prusachenko, P.S., Khryachkov, V.A., Ketlerov, V.V., Bokhovko, M.V., Bondarenko, I.P., 2018. Optimization of the n/γ separation algorithm for a digital neutron spectrometer. Nucl. Instrum. Methods Phys. Res. Sect. A 905, 160–170. https://doi.org/10.1016/j.nima.2018.07.062.

Sarkar, S., Bhairannawar, S.S., 2021. Efficient FPGA architecture of optimized Haar wavelet transform for image and video processing applications. Multidim Syst. Sign Process. 32, 821–844. https://doi.org/10.1007/s11045-020-00759-4.

Singh, H., Mehra, R., 2017. Discrete wavelet transform method for high flux *n*-γ discrimination with liquid scintillators. IEEE Trans. Nucl. Sci. 64, 1927–1933. https://doi.org/10.1109/TNS.2017.2708602.

Singh, H., Singh, S., 2015. Novel discrimination parameters for neutron-gamma discrimination with liquid scintillation detectors using wavelet transform. J. Inst. 10, P06014–P. https://doi.org/10.1088/1748-0221/10/06/P06014.

Söderström, P.-A., Nyberg, J., Wolters, R., 2008. Digital pulse-shape discrimination of fast neutrons and γ-rays. Nuclr Instrum. Meth. A 594, 79–89.

Tang, Y.Y., 2014. Haar Wavelet: Wavelet Theory Approach to Pattern Recognition, second ed. World Scientific Publishing Co PTE Ltd.

Winyard, R.A., Lutkin, J.E., McBeth, G.W., 1971. Pulse shape discrimination in inorganic and organic scintillators. I. Nucl. Instrum. Meth. 95, 141–153. https://doi.org/10.1016/0029-554X(71)90054-1.

Yang, Y., Liu, G.-F., Yang, J., Luo, X.-L., Meng, D.-Y., 2014. Digital discrimination of neutron and γ-ray using an organic scintillation detector based on wavelet transform modulus maximum. Chinese Phys. C 38, 36202. https://doi.org/10.1088/1674-1137/38/3/036202.

Yousefi, S., Lucchese, L., Aspinall, M.D., 2009. Digital discrimination of neutrons and gamma-rays in liquid scintillators using wavelets. Nucl. Instrum. Meth. A. 598, 551–555. https://doi.org/10.1016/j.nima.2008.09.028.

Zaitseva, N., Rupert, B.L., PaweŁczak, I., Glenn, A., Martinez, H.P., Carman, L., Faust, M., Cherepy, N., Payne, S., 2012. Plastic scintillators with efficient neutron/gamma pulse shape discrimination. Nucl. Instrum. Methods Phys. Res. A. 668, 88–93. https://doi.org/10.1016/j.nima.2011.11.071.